

Binary neutron stars in a waveless approximation

Kōji Uryū,¹ Fran ois Limousin,² John L. Friedman,³ Eric Gourgoulhon,² and Masaru Shibata⁴

¹ SISSA, via Beirut 4, 34014 Trieste, Italy

² Laboratoire de l'Univers et de ses Th ories, UMR 8102 du C.N.R.S.,

Observatoire de Paris, F-92195 Meudon Cedex, France

³ Department of Physics, University of Wisconsin-Milwaukee, P.O. Box 413, Milwaukee, WI 53201

⁴ Department of Earth Science and Astronomy, Graduate School of Arts and Sciences,

University of Tokyo, Komaba, Meguro, Tokyo 153-8902, Japan

(Dated: December 2, 2024)

Equilibria of binary neutron stars in close circular orbits are computed numerically in a waveless approximation to general relativity. The full Einstein equation is solved on an initial hypersurface to obtain an asymptotically flat form of the 4-metric and an extrinsic curvature whose time derivative vanishes in a comoving frame. Two independent numerical codes, one based on a finite difference method, the other on a spectral method, are developed, and solution sequences that model inspiraling binary neutron stars during the final several orbits are successfully computed. The binding energy of the system near its final orbit deviates from earlier results of third post-Newtonian and of spatially conformally flat calculations. The new solutions may serve as initial data for merger simulations and as members of quasiequilibrium sequences to generate gravitational wave templates, and may improve estimates of the gravitational-wave cutoff frequency set by the last inspiral orbit.

PACS numbers:

Introduction: Equilibria of close binary neutron stars in circular orbits, constructed numerically, have been studied as a model of the final several orbits of binary inspiral prior to merger (see [1] for a review). These numerical solutions have been used as initial data sets for merger simulations [2]; in quasi-equilibrium sequences, to estimate gravitational waveforms [3, 4]; and to determine the cutoff frequency of the inspiral waves [5, 6, 7].

To maintain equilibrium circular orbits in general relativity one must introduce an approximation that eliminates the back reaction of gravitational radiation. An ansatz of this kind is the waveless approximation proposed by Isenberg [8]. His approach adopts a constrained Hamiltonian formulation of Einstein's equation in which time derivatives of dynamical variables are discarded. As a result field equations for the metric components become elliptic equations. The gravitational field is no longer dynamical, and the dynamics of a system are determined by the equation of motion of the matter source. One of his proposals was to choose a conformally flat spatial geometry maximally embedded in a spacetime. Wilson and Mathews later rediscovered this type of waveless approximation and applied to numerical computations of binary inspirals [9]. The Isenberg-Wilson-Mathews (IWM) formulation has been widely used for modeling binary neutron star inspiral in the past decade [9, 10, 11, 12, 13] as well as to compute binary black hole solutions [14]. For applications of the IWM formulation to simulations, see [6, 15].

The error introduced in a solution by restriction to conformally flat three geometry was examined in Refs. [16, 17]. In models of binary neutron stars, it is estimated to cause a several percent error in the orbital angular velocity [3], implying a comparable deviation from circular

orbits [18].

New waveless formulations, incorporating a generic form of the metric, are suitable for accurate computation of binary compact objects[19, 20]. In this letter, we present first results of numerical computations for binary neutron stars modeled in one of these formulations [20].

Formulation of the waveless spacetime: The new formulation [20] exactly solves the Einstein-Euler system written in 3+1 form on a spacelike hypersurface. The spacetime $\mathcal{M} = \mathbb{R} \times \Sigma$ is foliated by the family of spacelike hypersurfaces, $\Sigma_t = \{t\} \times \Sigma$. The future-pointing normal n^α to Σ_t is related to the timelike vector t^α (the tangent ∂_t to curves $t \rightarrow (t, x)$, $x \in \Sigma$) by $t^\alpha = \alpha n^\alpha + \beta^\alpha$, where α is the lapse, and where the shift β^α satisfies $\beta^\alpha n_\alpha = 0$. A spatial metric $\gamma_{ab}(t)$ defined on Σ_t is equal to the projection tensor $\gamma_{\alpha\beta} = g_{\alpha\beta} + n_\alpha n_\beta$ restricted to Σ_t . In terms of a conformal factor ψ and a conformally rescaled spatial metric $\tilde{\gamma}_{ab} = \psi^{-4} \gamma_{ab}$, the metric $g_{\alpha\beta}$ takes the form, $ds^2 = -\alpha^2 dt^2 + \psi^4 \tilde{\gamma}_{ij}(dx^i + \beta^i dt)(dx^j + \beta^j dt)$, in a chart $\{t, x^i\}$. A condition to specify the conformal decomposition is $\det \tilde{\gamma}_{ab} = \det f_{ab}$, where f_{ab} is a flat metric.

In our formulation we impose, as coordinate conditions, maximal slicing ($K = 0$) and the spatially transverse condition $\mathring{D}_b \tilde{\gamma}^{ab} = 0$ (the Dirac gauge [20, 21]), where \mathring{D}_b is the covariant derivative with respect to the flat metric. We then restrict time-derivative terms in this gauge to guarantee that all components of the field equation are elliptic equations, and hence that all metric components, including the spatial metric, have Coulomb-type fall off [20]. While it is found to be sufficient to impose a condition, $\partial_t \tilde{\gamma}^{ab} = O(r^{-3})$, to have Coulomb-type fall off in the asymptotics, we impose a stronger condition $\partial_t \tilde{\gamma}^{ab} = 0$. For the other quantities, we impose heli-

cal symmetry: spacetime and fluid variables are dragged along by the helical vector $k^\alpha = t^\alpha + \Omega\phi^\alpha$. For example, the time derivative of extrinsic curvature K_{ab} is expressed as $\partial_t K_{ab} = -\mathcal{L}_{\Omega\phi} K_{ab}$. The resulting field equations are solved on a slice Σ_0 . The Hamiltonian constraint, momentum constraint, spatial trace and spatial tracefree part of the Einstein equation are, respectively, regarded as elliptic equations for ψ , β^a , α and $h_{ab} := \tilde{\gamma}_{ab} - f_{ab}$, while A_{ab} , the trace free part of the extrinsic curvature, is computed from the metric components.

To compute the motion of binary neutron stars in circular orbits, the flow field is assumed to be stationary in the rotating frame. Since any solution to the waveless formulation satisfies all constraint equations, it is, in particular, an initial data set for the Einstein-(relativistic)Euler system. When one evolves such a binary neutron star solution by integrating the Einstein-Euler system, the orbits will deviate from exact circularity because of the radiation reaction force. Instead, one can construct an artificial spacetime with circular orbits by dragging the waveless solution on Σ_0 along the helical vector, $k^\alpha = t^\alpha + \Omega\phi^\alpha$, so that the spacetime has helical symmetry. Although the spacetime so constructed will not exactly satisfy Einstein's equation, a family of such spacetimes, associated with circular orbits of decreasing separation, will model the inspiral of a binary neutron star system during its final several orbits. We expect this sequence of approximate solutions to be more accurate than earlier quasiequilibrium sequences obtained in the IWM framework. Explicit forms of all equations for the fields and the matter are found in [20, 21].

Numerical methods: We have developed two independent numerical schemes to compute binary neutron star solutions. One is based on a finite difference method [12], the other on a spectral method implemented via the C++ library LORENE [22]. Each method has been successfully used to compute binary neutron star configurations using the IWM formulation [11, 12, 13]. For the new waveless formulation, detailed convergence tests and calibration of each method will be published separately. In this letter, we show quantitative agreement of the two methods for h_{ab} , which is the significant and reliable calibration for the new numerical solutions.

In both methods, equations are written in Cartesian coordinate components, and they are solved numerically on spherical coordinate grids, r , θ , and ϕ . In the finite difference method, an equally spaced grid is used from the center of orbital motion to $5R_0$ where there are $n_r = 16$, 24, and 32 grid points per R_0 ; from $5R_0$ to 10^4R_0 a logarithmically spaced grid has 60, 90, and 120 points (depending on the resolution). Here R_0 is the geometric radius of a neutron star along a line passing through the center of orbit to the center of a star. Accordingly, for θ and ϕ there are 32, 48, and 64 grid points each from 0 to $\pi/2$ [12]. For the spectral method, five domains (a nucleus, three shells and a compactified domain extend-

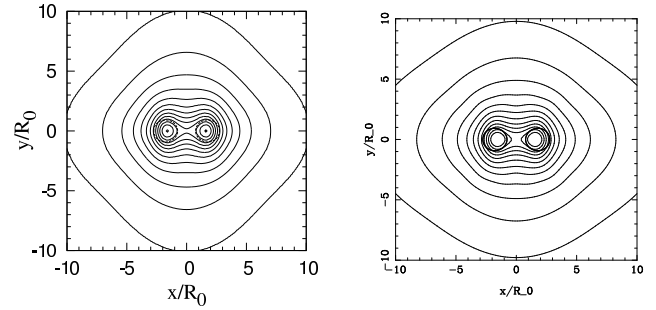


FIG. 1: Contours of $(h_{xx} - h_{yy})/2$ in the xy -plane, computed by the finite difference code (left) and by the spectral code (right). The binary separation $2d$ is given by $d/R_0 = 1.75$. Contours extend from -0.014 to -0.002 with step 0.001.

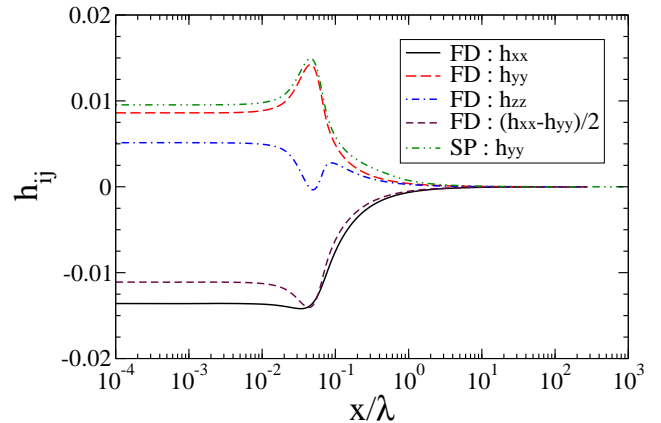


FIG. 2: Components h_{ij} along the x -axis, normalized by $\lambda = \pi/\Omega$. A neutron star extends from $x/\lambda = 0.02024$ to 0.04722 . Curves labeled FD and SP display results of the finite difference and spectral codes, respectively

ing up to infinity) around each star are used. In each domain, the number of collocation points is chosen to be $N_r \times N_\theta \times N_\phi = 33 \times 21 \times 20$ [11].

Numerical solutions for binary neutron stars: A model of the evolutionary path of binary inspiral is given by a sequence of equilibria along which the neutron star matter is assumed to be isentropic; and the implied fluid flow is assumed to conserve the baryon number, entropy and vorticity of each fluid element [23]. In the case where the spins of component stars are negligible, the flow becomes irrotational; one can introduce the velocity potential Φ by $hu_\alpha = \nabla_\alpha \Phi$, where h is the specific enthalpy and u^α is the fluid 4-velocity. For isentropic flow, one can assume a one-parameter equation of state, $p = p(\rho)$, with ρ the baryon mass density. The matter is then described by two independent variables, a thermodynamic variable such as p/ρ , and the velocity potential Φ . In this letter, we assume a polytropic equation of state $p = \kappa\rho^\Gamma$ with adiabatic index $\Gamma = 2$, and we display results for equal-mass binaries.

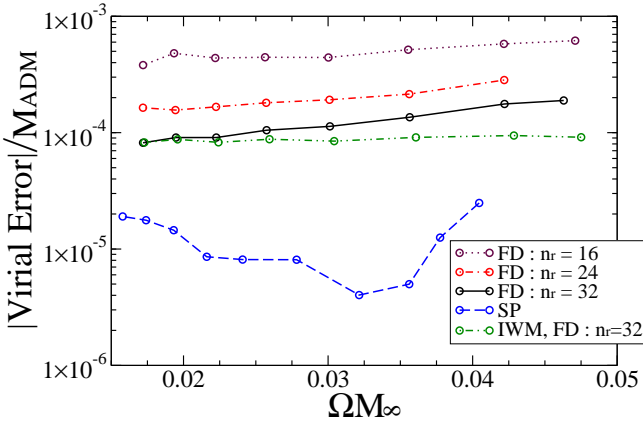


FIG. 3: Virial error vs. angular velocity Ω , normalized by M_∞ , twice the gravitational mass of an isolated neutron star. Each curve labeled FD shows results of a finite difference code with a given resolution. Curves labeled SP and IWM show results of the spectral code and the spatially conformally flat approximation, respectively.

In Fig. 1, contours of the non-conformal part of the metric computed by two numerical codes are shown for selected solutions. In these solutions, the rest mass of each star is taken to be that of a single spherical star of compactness $(M/R)_\infty = 0.17$, and the half separation in coordinate distance from the orbital center to the geometric center of a neutron star is set to $d/R_0 = 1.75$. From these contours, one can verify qualitative agreement of the results from the two independent numerical methods. In Fig. 2, components h_{ij} along the x -axis are plotted for the same solution, where the x -axis passes through the centers of the neutron stars.

In [20], it is shown that the ADM mass, M_{ADM} , and the asymptotic Komar mass, M_K defined by

$$M_{\text{ADM}} := \frac{1}{16\pi} \oint_\infty (\partial_b \gamma^{ab} - \partial^a \gamma_b^b) dS_a, \quad (1)$$

$$M_K := -\frac{1}{8\pi} \oint_\infty \nabla^\alpha t^\beta dS_{\alpha\beta} \quad (2)$$

are equal, $M_{\text{ADM}} = M_K$, under asymptotic conditions satisfied by solutions in the present formulation. The equality is related to a virial relation for the equilibrium,

$$\int x^a \gamma_a^\alpha \nabla_\beta T_\alpha^\beta \sqrt{-g} d^3x = 0, \quad (3)$$

which is used to examine accuracy of numerical solutions. Fig. 3 shows the computed value of the virial integral in Eq. (3), normalized by M_{ADM} , for a solution sequence with $(M/R)_\infty = 0.17$. The figure portrays the increase in accuracy of the finite difference method as the resolution increases from $n_r = 16$ to 32. We also evaluated the surface integrals Eqs. (1) and (2) on a sphere of large radius, centered at the binary system's center of mass.

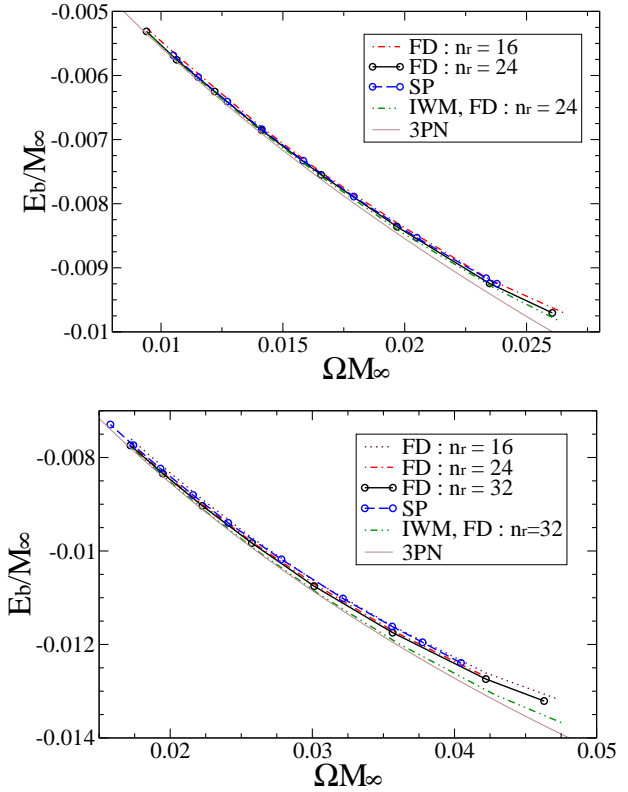


FIG. 4: Plot of the binding energy $E_b := M_{\text{ADM}} - M_\infty$ with respect to the normalized angular velocity for $(M/R)_\infty = 0.12$ (top) and 0.17 (bottom). Curves are labeled as in Fig. 3. The thin solid curve shows results from the 3PN calculation [24].

We confirmed that each mass converges asymptotically and that, for each model, the difference of the two masses is as small as $|M_{\text{ADM}} - M_K|/M_{\text{ADM}} \sim 0.01\%$ for the finite difference method and $\sim 0.001\%$ for the spectral method; these errors are consistent with the numerical errors of the virial relation shown in Fig. 3.

Finally, the binding energy $E_b = M_{\text{ADM}} - M_\infty$ of solution sequences for two models are plotted in Fig. 4. The top panel shows a less compact model with $(M/R)_\infty = 0.12$, the bottom panel a model whose compactness, $(M/R)_\infty = 0.17$, is closer to that of neutron stars. The thin solid curve in each figure describes a third post-Newtonian (3PN) calculation [24], and the dot-dot-dash curve describes solutions in the IWM formulation. For each compactness, our solution sequence fits the 3PN curve well at larger separation. Each sequence reaches a configuration with a cusp without any turning point in the binding energy curve, in agreement with results of the IWM formulation [12, 13] (the spectral code does not yet converge for the closest orbits – largest ΩM_∞ – of Figs. 3 and 4, because it is more sensitive to tidal deformation: higher multipoles in the density of each star lead to a divergent iteration). For the case with $(M/R)_\infty = 0.12$, the waveless solutions agree well with

the IWM solution; as expected, the contribution of h_{ab} is small for the smaller compactness. For the case with $(M/R)_\infty = 0.17$, however, the binding energy E_b of the waveless sequences clearly deviates from that of the 3PN and IWM sequences at the larger values of ΩM_∞ . This suggests that the 3PN and IWM formulations each overestimate the binding energy – in the 3PN case, by neglecting the tidal deformation, in the IWM formulation by neglecting the contribution from h_{ab} .

Discussion: According to the second post Newtonian theory (e.g. [16]), the correction to binding energy ΔE_b due to the contribution of h_{ij} is of order $M_\infty h_{ij} v^i v^j$, where the magnitude of orbital velocity, v^i , may be typically $v \approx 0.34(\Omega M_\infty/0.04)^{1/3}$. Since h_{ij} is of $O(v^4)$, $\Delta E_b/M_\infty = O(v^6) \sim 10^{-3}$ for $\Omega M_\infty \sim 0.04$. This agrees with the difference between the binding energies calculated by the IWM and waveless formulation in Fig. 4.

An important quantity for the data analysis of gravitational waves is $dE_b/d\Omega$, because it determines the evolution of gravitational wave phase $\Phi_{\text{GW}} = 2 \int \Omega(t) dt$. Assuming adiabatic evolution, the time dependence of angular velocity $\Omega(t)$ is calculated from $d\Omega/dt = |(dE/dt)_{\text{GW}}|/(dE_b/d\Omega)$, where $(dE/dt)_{\text{GW}}$ is the luminosity of gravitational waves. Our present result shows that the derivative $dE_b/d\Omega$ of waveless sequences is $\sim 10\text{--}15\%$ larger than those of IWM and 3PN curves for $\Omega M_\infty \gtrsim 0.035$. Since ~ 2 orbits are maintained from $\Omega M_\infty = 0.035$ to merger for the case with $(M/R)_\infty = 0.17$ [3], the error in Φ_{GW} calculated from the equilibrium sequence of IWM and 3PN formulations would be accumulated to $\sim 50\%$ during the last ~ 2 orbits. The error may not be negligible for accurately determining the frequency of gravitational waves at the final orbits before merger, which can be used for constraining equations of state for nuclear matter [6, 7, 25].

Such a phase error may be much larger for the final orbits of binary black hole and black hole–neutron star inspirals. In these cases, ΩM_∞ in the last orbit may reach ~ 0.1 or larger (e.g. [14, 24]). Since ΔE_b is of order $O(v^6)$, the phase error is likely to be of order unity around $\Omega M_\infty \gtrsim 0.1$. Therefore, a template constructed from the IWM formulation may cause a systematic error in the data analysis. Our waveless approximation may improve binary black hole and black hole–neutron star solutions for this purpose.

Acknowledgement: This work was supported by Monbukagakusho Grant (17030004 and 17540232), and NSF grant PHY 0071044. KU thanks l’Observatoire de Paris for a visiting program in May 2004 and Nobuyuki Kanda for visiting Osaka City University, March 2005.

[1] T.W. Baumgarte and S.L. Shapiro, Phys. Rep. **376**, 41 (2003).

[2] e.g. M. Shibata and K. Uryū, Phys. Rev. D **61**, 064001 (2000); M. Shibata, K. Taniguchi and K. Uryū, Phys. Rev. D **68**, 084020 (2003); ibid. D **71**, 084021 (2005).

[3] M. Shibata and K. Uryū, Phys. Rev. D **64**, 104017 (2001).

[4] M. D. Duez, T. W. Baumgarte, S. L. Shapiro, M. Shibata, and K. Uryū Phys. Rev. D, **65**, 024016 (2002).

[5] J. A. Faber, P. Grandclement, F. A. Rasio and K. Taniguchi, Phys. Rev. Lett. **89**, 231102 (2002).

[6] R. Oechslin, K. Uryū, G. Poghosyan, and F. K. Thielemann, Mon.Not.Roy.Astron.Soc., **349**, 1469 (2004).

[7] M. Bejger, D. Gondek-Rosinska, E. Gourgoulhon, P. Haensel, K. Taniguchi, and J. L. Zdunik, Astron. Astrophys. **431**, 297 (2005).

[8] J. Isenberg, *Waveless Approximation Theories of Gravity*, preprint University of Maryland (1978); J. Isenberg and J. Nester, in *General Relativity and Gravitation* Vol.1, edited by A. Held, (Plenum Press, New York 1980).

[9] J. R. Wilson and G. J. Mathews, Phys. Rev. Lett. **75**, 4161 (1995); P. Marronetti, G. J. Mathews and J. R. Wilson, Phys. Rev. D **60**, 087301 (1999).

[10] T. W. Baumgarte, G. B. Cook, M. A. Scheel, S. L. Shapiro and S. A. Teukolsky, Phys. Rev. D **57**, 6181 (1998); *ibid* **57**, 7299 (1998).

[11] S. Bonazzola, E. Gourgoulhon and J.-A. Marck, Phys. Rev. Lett. **82**, 892 (1999); E. Gourgoulhon, P. Grandclément, K. Taniguchi, J.-A. Marck, S. Bonazzola, Phys. Rev. D **63** (2001) 064029.

[12] K. Uryū and Y. Eriguchi, Phys. Rev. D. **61**, 124023 (2000); K. Uryū, M. Shibata and Y. Eriguchi, Phys. Rev. D **62**, 104015 (2000).

[13] K. Taniguchi and E. Gourgoulhon, Phys. Rev. D **66**, 104019 (2002); *ibid*. Phys. Rev. D **68**, 124025 (2003).

[14] E. Gourgoulhon, P. Grandclément, and S. Bonazzola, Phys. Rev. D **65**, 044020 (2002); P. Grandclément, E. Gourgoulhon, and S. Bonazzola, Phys. Rev. D **65**, 044021 (2002); G.B. Cook and H. P. Pfeiffer, Phys. Rev. D **70**, 104016 (2004).

[15] J. A. Faber, P. Grandclément, and F. A. Rasio, Phys. Rev. D, **69**, 124036 (2004).

[16] H. Asada, M. Shibata, T. Futamase, Prog. Theor. Phys. **96**, 81, (1996); H. Asada and M. Shibata, Phys. Rev. D **54**, 4944 (1996).

[17] G. B. Cook, S. L. Shapiro, and S. A. Teukolsky Phys. Rev. D **53**, 5533 (1996); W. Kley, and G. Schäfer, Phys. Rev. D **60**, 027501 (1999); A. Garat, and R. H. Price, Phys. Rev. D **61**, 124011 (2000).

[18] T. Mora, C. M. Will, Phys. Rev. D **69**, 104021 (2004); M. Miller, P. Gressman, and W.-M. Suen Phys. Rev. D **69**, 064026 (2004); M. Miller, Phys. Rev. D **69**, 124013 (2004); P. Marronetti, M. D. Duez, S. L. Shapiro and T. W. Baumgarte Phys. Rev. Lett. **92**, 141101 (2004).

[19] G. Schäfer and A. Gopakumar, Phys. Rev. D **69**, 021501(R) (2004).

[20] M. Shibata, K. Uryū, and J. L. Friedman, Phys. Rev. D **70**, 044044 (2004); Erratum *ibid*. **70**, 129901(E) (2004).

[21] S. Bonazzola, E. Gourgoulhon, P. Grandclément, J. Novak, Phys. Rev. D **70**, 104007 (2004).

[22] <http://www.lorene.obspm.fr>

[23] C. S. Kochanek, Astrophys. J. **398**, 234 (1992); L. Bildsten and C. Cutler, Astrophys. J. **400**, 175 (1992).

[24] L. Blanchet, Phys. Rev. D **65**, 124009 (2002).

[25] X. Zhuge, J. M. Centrella, S. L. W. McMillan, Phys. Rev. D **50**, 6247 (1994).